

# Optimization of a Landfill Gas Collection Shutdown Based on an Adapted First-Order Decay Model

1 *Daniel A. Lagos<sup>a</sup>, Martin Héroux<sup>b</sup>, Ryan Gosselin<sup>c</sup> and Alexandre R. Cabral<sup>d,\*</sup>*

2 *<sup>a</sup>Engineer, Biothermica Technologies Inc., Montreal, QC, Canada. Formerly with*  
3 *Centre Universitaire de Formation en Environnement (CUFE), Université de*  
4 *Sherbrooke, Sherbrooke, QC, Canada . [daniel.lagos@usherbrooke.ca](mailto:daniel.lagos@usherbrooke.ca)*

5 *<sup>b</sup>Engineer, City of Montreal, Montreal, QC, Canada. [mheroux@ville.montreal.qc.ca](mailto:mheroux@ville.montreal.qc.ca)*

6 *<sup>c</sup> Associate Professor, Department of Chemical Engineering, Université de Sherbrooke,*  
7 *Sherbrooke, QC, Canada J1K 2R1. [ryan.gosselin@usherbrooke.ca](mailto:ryan.gosselin@usherbrooke.ca)*

8 *<sup>d</sup> Professor, Department of Civil Engineering, Université de Sherbrooke, Sherbrooke,*  
9 *QC, Canada J1K 2R1. [alexandre.cabral@usherbrooke.ca](mailto:alexandre.cabral@usherbrooke.ca)*

10

11 *\* Corresponding Author*

12

Lagos, D.A., Héroux, M.#, Gosselin, R. and Cabral, A.R. (2017). Optimization of a landfill gas collection shutdown based on an adapted first-order decay model. Waste Management, 63: 238-245. <http://dx.doi.org/10.1016/j.wasman.2016.08.012>

13 **ABSTRACT**

14 LandGEM's equation was reformulated to include two types of refuse, fast decaying refuse  
15 (*FDR*) and slow decaying refuse (*SDR*), whose fractions and key modeling parameters  $k$   
16 and  $L_0$  were optimized independently for three periods in the life of the Montreal-CESM  
17 landfill. Three scenarios were analyzed and compared to actual biogas collection data: 1)  
18 Two-Variable Scenario, where  $k$  and  $L_0$  were optimized for a single type of refuse; 2) Six-  
19 Variable Scenario, where three sets of  $k$  and  $L_0$  were optimized for the three periods and  
20 for a single type of refuse; and 3) Seven-Variable Scenario, whereby optimization was  
21 performed for two sets of  $k$  and  $L_0$ , one associated with *FDR* and the second with *SDR*, and  
22 for the fraction of *FDR* during each of the three periods. Results showed that the lowest  
23 error from the error minimization technique was obtained with the Six-Variable Scenario.  
24 However, this scenario's estimation of gas generation was found to be rather unlikely. The  
25 Seven-Variable Scenario, which allowed for considerations about changes in landfilling  
26 trends, offered a more reliable prediction tool for landfill gas generation and optimal  
27 shutdown time of the biogas collection system, when the minimum technological threshold  
28 would be attained. The methodology could potentially be applied *mutatis mutandis* to other  
29 landfills, by considering their specific waste disposal and gas collection histories.

30

31 **KEYWORDS:** Landfill gas collection; First-order decay model; LandGEM; IPCC  
32 model; Fast-decaying refuse; Slow-decaying refuse

33

## 34 INTRODUCTION

35 When landfill methane ( $\text{CH}_4$ ) generation reaches a critical low value, the system employed  
36 to burn biogas must be replaced or, conditions permitting, shut down. The decision-making  
37 process is challenging because of the difficulty in predicting relatively accurate future  
38 trends sufficiently in advance. This is the type of challenge being faced by the operator of  
39 the Montreal CESM landfill. This 72-ha site, which accepted refuse from 1968 to 2008, is  
40 located in a former limestone quarry, in a (now) densely populated area of Montreal. The  
41 depth of refuse reaches 80 m in certain areas, and it is estimated that some 40 million tons  
42 of refuse from various origins were landfilled at the CESM landfill site. Prior to the  
43 beginning of the landfill operations, the bottom and side walls of the former quarry were  
44 not impermeabilized. As a consequence, most of the waste mass is virtually saturated. The  
45 database for this site included 41 years of landfilling data and a compilation of daily entries  
46 of 20 years of biogas collection data.

47 Current methods to predict landfill gas generation include first-order decay U.S. EPA's  
48 Landfill Gas Emissions Model (LandGEM) (USEPA, 2005), which considers only one  
49 type of municipal solid waste (MSW) for the entire lifetime of a site. The two key  
50 parameters in LandGEM are  $L_0$ , which represents the methane production potential ( $\text{m}^3$   
51  $\text{Mg}^{-1}$  wet waste) and  $k$ , which represents the first-order decay rate associated with waste  
52 decomposition ( $\text{yr}^{-1}$ ) (USEPA, 2005). Some models, such as the one proposed by the  
53 Intergovernmental Panel on Climate Change (IPCC, 2006), allow for a multiphase refuse  
54 input, which could potentially lead to more precise predictions. However, a common  
55 predicament in landfill management is the lack of information regarding landfilling history

56 and/or lack of specific data about refuse categories and subcategories. This is particularly  
57 true for old sites, such as the CESM landfill, which had no guidelines or regulations  
58 regarding keeping track of the nature of admitted refuse. This study proposes a  
59 methodology of reformulation of a first-order model. It aims at improving model predictive  
60 performance using available information about the history of the site and gas collection  
61 data.

62 In the past 2 decades, societal changes in landfilling practices have occurred as a result of  
63 stricter legislation, improvements in recycling, higher raw material value, etc. One  
64 important example of legislation-driven change is the imposed reduction in landfilling of  
65 organic matter in the European Union (Directive 1999/31/EC). Quebec's (Canada) recent  
66 governmental policy ("Quebec Residual Materials Management Policy") is now calling for  
67 the banishment of organic matter in landfills in this province by the year 2020. Changes in  
68 waste characteristics need to be taken into account in biogas generation modeling; for  
69 example, by using values of  $k$  and  $L_0$  that evolve throughout the site's history. The first  
70 important characteristic of the proposed methodology was therefore the subdivision of the  
71 lifetime of the CESM landfill into 3 distinct periods – 1968-1989 / 1990-1999 / 2000-2008  
72 – that reflect the specific history of refuse admittance, i.e. changes in the characteristics of  
73 the wastes. As mentioned previously, while data about quantities landfilled could be found  
74 for the entire lifetime of the site, specific data about refuse categories were not available.

75 It is proposed to distinguish herein two distinct categories of landfill refuse, namely fast  
76 decaying refuse (*FDR*) and slow decaying refuse (*SDR*). For instance, as per IPCC-  
77 recommended  $k$  values, food waste in MSW having a high value of  $k$  was segregated as  
78 *FDR*, whereas materials whose  $k$  values are low, such as wood-straw waste, were assigned

79 to the *SDR* category. The specific segregation of refuse in either *FDR* or *SDR* is presented  
80 in Table 1. Based on the  $k$  value, once a type of waste was categorized as either *FDR* or  
81 *SDR*, its minimum and maximum  $L_0$  values (given as mass of degradable organic carbon;  
82 DOC) were assigned following IPCC (2006) recommendations for this type of waste.  
83 Given the lack of precise information about the characteristics of the waste, it was decided  
84 to limit segregation of the bulk waste to these two main categories.

85 According to IPCC-recommended  $L_0$  and  $k$  values (IPCC, 2006), *FDR* can be characterized  
86 by low values of  $L_0$  and fast kinetics (high values of  $k$ ), while *SDR* is characterized by high  
87 methane generation potentials (high values of  $L_0$ ) and slow kinetics (low values of  $k$ ). These  
88 considerations about  $k$  and  $L_0$  values are generalizations of the observed tendencies in  
89 IPCC-recommended  $k$  and  $L_0$  values and are representative of the bulk behaviour of the  
90 waste mass and not that of specific components. This approximation results in the  
91 overlapping of *FDR* and *SDR*  $L_0$  values, as discussed when presenting the data in Table 2.  
92 It is considered herein that a decrease in the quantity of landfilled *FDR* results in a decrease  
93 of the bulk mass'  $k$  value and an increase in  $L_0$ . An important caveat is given by Wang et  
94 al. (2011) (Wang et al., 2011), who have shown that component-specific low decay rates  
95 among species of wood do not necessarily correlate with high methane yields. In this study,  
96 the magnitude of the variation in  $L_0$  is a resultant of the optimization technique, which sets  
97  $L_0$  within IPCC-recommended ranges.

98

99 Table 1 - Segregation of *FDR* and *SDR* and corresponding  $k$  values as per IPCC  
100 recommended ranges. Adapted from IPCC (2006).

101

102 These adaptations of the biogas generation modeling process were considered in order to  
103 develop a more reliable management tool to predict landfill gas generation. So far,  
104 LandGEM has been used at the CESM landfill.

105 By attributing independent values of  $k$  and  $L_0$  and different fractions between  $FDR$  and  
106  $SDR$  that best reflected the changing proportions of admitted refuse during the 3 periods  
107 mentioned previously, the same first-order model equation used in LandGEM was adapted  
108 to generate production curves. Minimization of error between modeled generation and  
109 generated gas helped to find the best fitting curve, i.e. the optimized values of  $k$ ,  $L_0$ , and  
110 fraction of  $FDR$  for each period. In an intermediate step, collection data were transformed  
111 into generation data by adopting a fixed recovery efficiency rate.

112 The objective is to use the optimized generation curves to predict the optimal moment to  
113 shut down the biogas collection system, when the minimum technological threshold (MTT)  
114 would be attained. The optimized values of the independent variables were tested against  
115 the known history of refuse admittance. In principle, the methodology adopted could be  
116 replicated to other landfills, by considering the specific evolution of the  $FDR$  fraction in  
117 the landfilled waste and the available gas collection database.

118

## 119 **METHODS**

### 120 **Landfill gas collection and landfilled mass data**

121 Landfill gas (LFG) collection data were obtained between 1994 and 2013. For this period,  
122 yearly compilations were performed using daily biogas collection data. A global relative  
123 error of 2.9% was calculated for the flowmeter and chromatograph used to measure  
124 collected CH<sub>4</sub> at the CESM landfill (Lagos, 2014). The total landfilled mass was  
125 determined on a yearly basis starting in the opening year, in 1968, until its closure, in 2008.  
126 The types of refuse admitted were mainly household, commercial, institutional and  
127 industrial waste, as well as construction and demolition debris. The latter included inert  
128 (non LFG-generating) matter such as, asphalt, concrete and bricks.

#### 129 **Transformation from gas collection to generation data**

130 Gas collection data were transformed into generation data by setting a recovery efficiency  
131 percentage that remained constant throughout the lifetime of the site. The main analysis  
132 (presented in detail herein) was performed with an efficiency rate considered as excellent  
133 in the literature, i.e. 75% (Spokas et al., 2006; Spokas et al., 2015). Given the proximity of  
134 this landfill to housing developments, the presence of an extensive active gas collection  
135 system (consisting of over 260 LFG collection wells), and a history of very low measured  
136 emissions, high efficiencies can be considered plausible for this specific site (Franzidis et  
137 al., 2008; Héroux et al., 2010). According to IPCC (2006), higher than 75% collection  
138 efficiencies can only be attributed to properly capped sites with well-designed and well-  
139 operated gas recovery systems. In order to evaluate how the year of occurrence of MTT is  
140 affected by gas collection efficiency, MTT was obtained for the following recovery  
141 efficiency values: 55%, 65%, 75%, 85%, and 95%.

142

143 **Scenarios considered**

144 Based on refuse admittance history at CESM – including the ban of landfill organic matter  
145 in 2000 – and societal changes triggered by new recycling policies, the lifetime of this site  
146 was subdivided into 3 distinct periods: 1968–1989, 1990–1999 and 2000–2008. The  
147 extension of period 3 beyond the end of landfilling (2008) is justified by the need to predict  
148 methane generation to estimate the year of occurrence of MTT and the onset of aftercare.  
149 The beginning of period 3 was easily determined; it coincided with the ban on organic  
150 matter (*FDR*) admittance at CESM, in May 2000. The beginning of period 2 was chosen  
151 based on the implementation of recycling programs in the Province of Quebec in the early  
152 1990s. Given the fact that it is difficult to identify exactly when recycling programs became  
153 effective – therefore affecting the fractions of landfilled *FDR* and *SDR* –, the sensitivity of  
154 the transition between periods 1 and 2 was tested by setting it 4 years before and 4 years  
155 after 1990. This test was performed only for the Seven-Variable Scenario (presented  
156 hereafter).

157 Refuse admitted in each of the three periods had particular characteristics that distinguished  
158 it. Therefore, the fractions of landfilled *FDR* and *SDR* eventually became one of the  
159 variables of this parametric study, which was performed based on the following three  
160 scenarios, illustrated in Figure 1: 1) Two-Variable Scenario, for which one single set of the  
161 parameters  $k$  and  $L_0$  characterized the refuse for the entire lifetime of the site. This scenario  
162 corresponds to the current simple phase formulation of LandGEM; 2) Six-Variable  
163 Scenario, for which one set of  $k$  and  $L_0$  values would be selected for the refuse in each of  
164 the three key periods; and 3) Seven-Variable Scenario, for which two sets of  $k$  and  $L_0$  values  
165 were adopted: one characterizing *FDR* and the other *SDR*. Both sets remained the same



166 throughout the entire study period. However, 3 fractions of *FDR* in the refuse were adopted,  
167 one for each of the 3 key periods. All variables in these 3 scenarios were optimized within  
168 predetermined ranges as per IPCC (2006) recommendations.

169 It is obvious that a simple increase in the number of independent variables would lead to  
170 an improvement in model fit. But this would be meaningless if the optimization process  
171 did not include considerations about what really happened during the history of this  
172 landfill, in particular concerning the characteristics of the wastes landfilled. For example,  
173 an optimization result indicating that the site saw an increase in *FDR* over time would not  
174 be coherent with the fact that there was a ban in landfilling of organic matter at the  
175 beginning of period 3. Such an optimization result would therefore have to be rejected. In  
176 short, the 2, 6 or 7 variables in each model are not truly independent as each model must  
177 be both internally consistent (i.e. the relative value of each variable must be plausible) and  
178 correspond to reality.

179

180 Figure 1 - Schematic of the three scenarios and their corresponding variables.

181

## 182 **Modeling variables and their optimization ranges**

183 As shown in Figure 1, variables were labeled in the following manner: 1)  $k$  and  $L_0$ , for the  
184 Two-Variable Scenario; 2)  $k_1, k_2, k_3, L_{01}, L_{02}$  and  $L_{03}$ , for the Six-Variable Scenario; and 3)  
185  $L_0\text{-FDR}, L_0\text{-SDR}, k\text{-FDR}, k\text{-SDR}, f_1\text{-FDR}, f_2\text{-FDR}$  and  $f_3\text{-FDR}$ , for the Seven-Variable

186 Scenario. The subscript  $n = 1, 2$  or  $3$  denotes the landfilling period to which the variable  
187 belongs, while  $f_1, f_2$  and  $f_3$  denote the fractions of  $FDR$  in the refuse.

188 The ranges within which  $k, L_0, k_n, L_{0n}$  and  $f_n-FDR$  could vary during optimization were  
189 chosen to allow maximum flexibility while keeping values within IPCC recommended  
190 ranges and realistic in relation to the documented landfilling history. Optimization ranges  
191 for  $k$  and  $L_0$  were based on IPCC recommended values for  $FDR$  (i.e. food and municipal  
192 sludge) and  $SDR$  (i.e. cellulose and textiles) (IPCC, 2006). Values for  $k$  were taken from  
193 the Very Humid Tropical Climate category. This is assumed to be valid, since the CESM  
194 landfill is situated in an old quarry, with considerable influx of groundwater (H eroux,  
195 2008).  $L_0$  values, expressed as  $DOC$ , were converted into  $L_0$  using equation 1, as follows:

$$196 \quad L_0 = F \text{ DOC } DOC_f \left( \frac{16}{12} \right) MCF \quad (1)$$

197 where  $F$  is the fraction of  $CH_4$  in generated landfill gas;  $DOC_f$  is the fraction of dissimilated  
198 organic carbon;  $16/12$  is the molecular weight ratio of  $CH_4$  to C and  $MCF$  is the correction  
199 factor for aerobic decomposition (IPCC, 2006; Thompson et al., 2009).

200 The value of  $F$  was averaged at 0.56 from daily measurements of  $CH_4$  and  $CO_2$  in the  
201 collected landfill gas at CESM between 2001 and 2013.  $DOC_f$  was set at 0.5 (default value  
202 according to IPCC) and  $MCF$  at 1.0, as recommended by IPCC (2006) for a site under  
203 anaerobic conditions, such as the CESM landfill. Mass units of  $DOC$  were then converted  
204 to volumetric units using a  $CH_4$  volumetric mass of  $714 \text{ g m}^{-3}$ . While recent work by Wang  
205 et al. (2011) shows that  $DOC_f$  can significantly vary with the nature of waste, the default

206 IPCC value of 0.5 is considered constant in this study. This fact may be of interest in future  
207 studies in order to reduce uncertainties in the transformation of *DOC* to  $L_0$ .

208 Table 2 presents  $k$  and  $L_0$  optimization ranges for the three scenarios. The choice – among  
209 IPCC recommendations – of what is considered a very high  $k$  value for a North American  
210 landfill is partly justified by the high degree of saturation of the refuse. Furthermore, work  
211 by De la Cruz and Barlaz (2010) shows that component-specific IPCC-recommended  $k$   
212 values for food waste and garden-park waste were underestimated by 200% and 400%  
213 respectively. Wang et al. (2013) also concluded that higher values than usually  
214 recommended in the literature can be adopted in certain cases.

215 The ranges of values for each of the two categories of waste of the Seven-Variable Scenario  
216 (*FDR* and *SDR*) were also taken from IPCC (2006). The optimization range of  $L_0$   
217 corresponds to the minimum and maximum  $L_0$  found for the same waste categories  
218 considered in *FDR* and *SDR* segregation. The maximum and minimum values of  $k$  and  $L_0$   
219 for each category of waste were selected to create a single optimization range. It can be  
220 observed that there is some degree of overlapping of *FDR* and *SDR*  $L_0$  values between 105  
221 and 115 m<sup>3</sup> CH<sub>4</sub> Mg<sup>-1</sup>. In other words, the subdivision into *FDR* and *SDR* is not clear-cut.  
222 As mentioned previously, this overlap can be attributed to the generalizations of the trends  
223 observed in IPCC-recommended  $k$  and  $L_0$  values, which are representative of the bulk  
224 behaviour of the waste mass and not that of specific components.

225

226 Table 2 -  $k$  and  $L_0$  optimization ranges for the Two-, Six- and Seven-Variable Scenarios

227 (Based on IPCC (2006) values).

228

229 The *FDR* fractions of the Seven-Variable Scenario were estimated for each of the three  
230 periods. For period 2, *FDR* = 56% and *SDR* = 44%. These estimates were based on a study  
231 that characterized refuse landfilled in 2000, in the Province of Quebec (RECYC-QUÉBEC,  
232 2000). For period 3, based on a characterization study performed at the CESM site in 2006  
233 (Baillargeon et al., 2006), fractions for *FDR* and *SDR* were set at 5% and 95% respectively.  
234 Since the contribution of inert matter – such as concrete, asphalt and bricks – in generating  
235 LFG is, for all practical purposes, negligible, it was taken out of the mass balance when  
236 calculating *FDR* and *SDR* fraction estimates. For period 1, no characterization study could  
237 be found relating to *FDR* or *SDR* fractions. Nonetheless, it was expected that before period  
238 2, when recycling had yet to become common practice, a smaller fraction of *FDR* was  
239 landfilled (indeed, greater quantities of paper and cardboard ended up in the landfill). Based  
240 on available information, an estimated fraction of 25% was therefore adopted for *FDR* in  
241 period 1. Figure 2 shows the variation of these values throughout the lifespan of the site.

242 **Erreur ! Source du renvoi introuvable.** presents the optimization ranges for *FDR*  
243 fractions in the Seven-Variable Scenario. The adopted optimization range for the *FDR*  
244 fraction is wide, since it reflects the uncertainty resulting from lack of information for this  
245 site, and the estimative nature of characterization studies. Nonetheless, it is worthwhile  
246 repeating that the results must be anchored in reality. They must reflect the actual history  
247 of landfilling; otherwise, this study would be a mere fitting exercise.

248

249 Figure 2 - Schematic representation of the evolution of estimated *FDR* and *SDR* fractions  
250 at CESM from opening (1968) to closure (2008).

251

252 Table 3 - Optimization ranges for *FDR* fractions in the Seven-Variable Scenario for the  
253 three periods considered.

254

### 255 **LandGEM formulation**

256 LandGEM is based on the following first-order decomposition rate equation:

$$257 \quad Q_{CH_4n} = \sum_{i=1}^n \sum_{j=0.1}^1 k L_0 \left( \frac{M_i}{10} \right) e^{-kt_{i,j}} \quad (2)$$

258 where  $Q_{CH_4n}$  = annual methane generation in the  $n^{th}$  year of the calculation ( $m^3 \text{ yr}^{-1}$ );  $k$  =  
259 methane generation rate ( $\text{yr}^{-1}$ );  $L_0$  = potential methane generation capacity ( $m^3 \text{ Mg}^{-1}$ );  $M_i$  =  
260 mass of waste accepted in the  $i^{th}$  year ( $\text{Mg}$ );  $t_{ij}$  = age of the  $j^{th}$  section of waste mass  $M_i$   
261 accepted in the  $i^{th}$  year (decimal years);  $i$  = 1 year time increment;  $j$  = 0.1 year time  
262 increment; and  $n$  = number of years in the calculation, i.e. year of calculation – initial year  
263 of waste acceptance (USEPA, 2005).

264 For the Six- and Seven-Variable Scenarios, LandGEM calculations were rewritten in an  
265 Excel spreadsheet to be able to assign different sets of variables to each of the three periods.

### 266 **Error minimization technique**

267 The sum of squared errors (SSE) between gas collection data and modeled results was  
268 minimized by means of the Generalized Reduced Gradient nonlinear method using a  
269 commercial spreadsheet. The SSE is described by equation 3, as follows:

$$270 \quad SSE = \sum_{i=1}^n (Q_{mi} - Q_{ci})^2 \quad (3)$$

271 where  $n$  = number of yearly values of available collection data;  $i$  = year of calculation;  $Q_{mi}$   
272 = measured generated methane in the  $i^{th}$  year ( $\text{m}^3 \text{ yr}^{-1}$ ); and  $Q_{ci}$  = generated methane in the  
273  $i^{th}$  year calculated by equation 2 ( $\text{m}^3 \text{ yr}^{-1}$ ).

274 The unicity of the optimized results presented herein was evaluated by scanning the model  
275 variables within predetermined limits and computing SSE values for each set of selected  
276 parameters. This is illustrated in Figure 3, which presents the SSE values for  $10^4$   
277 combinations of  $k$  and  $L_0$  values ( $100 \times 100$ ) of the Two-Variable Scenario, for recovery  
278 efficiencies equal to 55%, 75% and 95%. The minimal SSE is found in the region  
279 represented by the darkest zone, which was set by an error range within 10% of the SSE.  
280 This zone confirms the presence of a single localized minimum. Similar behaviour was  
281 obtained for the Six- and Seven-Variable Scenarios.

282

283 Figure 3 – Model-predicted errors for the Two-Variable Scenario as function of recovery  
284 efficiency.

285

## 286 **RESULTS AND DISCUSSIONS**

287 Figure 4 shows CH<sub>4</sub> generation obtained by the reformulated LandGEM equation, for the  
288 three scenarios considered. The curve with solid points represents data collected from 1994  
289 to 2013 that were transformed into generation values by considering 75% recovery  
290 efficiency. The lowest SSE value was obtained for the Six-Variable Scenario. Accordingly,  
291 the best fit with generation data (based on actual collection) was obtained for this scenario.  
292 It was followed by the Seven-Variable and Two-Variable Scenarios with respective SSE  
293 values 2.6 and 6.3 times higher.

294

295 Scenarios were analyzed in terms of their ability to predict when the MTT would be  
296 attained. In the case of the CESM landfill facility, MTT is approximately 10 Mm<sup>3</sup> yr<sup>-1</sup>.  
297 Below this value, LFG collection would no longer be sustainable with the present gas  
298 collection system.

299

300 Figure 4 - Modeled CH<sub>4</sub> generation for the Two-, Six- and Seven-Variable Scenarios as  
301 optimized after SSE minimization relative to measured CH<sub>4</sub> generation.

302

### 303 **Two-Variable Scenario**

304 This scenario considers a single type of refuse admitted throughout the landfill's operating  
305 life. According to this scenario, the MTT would be reached in 2017. Based on latest  
306 available data (2012 and 2013), CH<sub>4</sub> generation seems to be underestimated.

307 Values of  $k$  and  $L_0$  optimized by SSE minimization were  $0.197 \text{ yr}^{-1}$  and  $127 \text{ m}^3 \text{ CH}_4 \text{ Mg}^{-1}$   
308 respectively. The relatively high  $k$  and low  $L_0$  would indicate a refuse with a high  
309 proportion of  $FDR$ , which is not necessarily the case for the refuse landfilled at the CESM  
310 site. This is an indication that this model does not coincide with actual landfill history and  
311 therefore needs refining.

### 312 **Six-Variable Scenario**

313 This scenario also considers a single type of refuse but landfilling was subdivided into the  
314 three periods indicated in **Erreur ! Source du renvoi introuvable.**; each with its own  
315 independently optimized values of  $k$  and  $L_0$ . Since the optimization ranges for  $k$  and  $L_0$   
316 were the same for all three periods, these variables were free to increase or decrease from  
317 one period to the next.

318 Optimized values for  $k_1, k_2, k_3, L_{01}, L_{02}$  and  $L_{03}$  were  $0.282 \text{ yr}^{-1}, 0.081 \text{ yr}^{-1}, 0.030 \text{ yr}^{-1}, 194$   
319  $\text{m}^3 \text{ CH}_4 \text{ Mg}^{-1}, 241 \text{ m}^3 \text{ CH}_4 \text{ Mg}^{-1}$  and  $21 \text{ m}^3 \text{ CH}_4 \text{ Mg}^{-1}$  respectively. The decrease in  
320 optimized  $k$  values – and increase in  $L_0$  values – between periods 1 and 2 implies that the  
321 fraction of  $FDR$  within the waste would also have decreased. Yet this is not corroborated  
322 by historical data. Indeed, recycling programs deployed in the early 1990s led to an  
323 important decrease in landfilling of paper and cardboard ( $SDR$  fraction), which caused an  
324 increase in the fraction of  $FDR$  in subsequent years (Figure 2).

325 Values of optimized  $L_0$  decreased between periods 2 and 3, implying that the fraction of  
326  $SDR$  would also have decreased. Again, this trend is not backed up by the CESM landfilling  
327 history. In 2000, CESM forbade admission of  $FDR$ , such as household waste, hence  
328 increasing  $SDR$  fractions. These mismatches between optimization of the variables and



329 known refuse admittance history suggest that the Six-Variable Scenario could not be  
330 retained, despite the fact that the lowest SSE value was obtained with it. Furthermore,  
331 before 1992 the modeled curve seems to greatly overestimate CH<sub>4</sub> generation in  
332 comparison with the other two scenarios with a ~ 100 Mm<sup>3</sup> difference at generation peak  
333 in 1990. Such an additional volume of landfill gas seems unlikely given the environmental  
334 nuisances that would have resulted for workers and the surrounding population; a nuisance  
335 that was never observed. Accordingly, the Six-Variable Scenario was deemed  
336 inappropriate to explain the behaviour of LFG generation for this site. According to the  
337 Six-Variable Scenario, the MTT would be reached in 2028.

### 338 **Seven-Variable Scenario**

339 This scenario considers two types of refuse and their fractions that vary along the three  
340 periods indicated in **Erreur ! Source du renvoi introuvable.**. Since the optimization  
341 ranges for the *FDR* fractions shown in **Erreur ! Source du renvoi introuvable.** are  
342 different but overlap between periods 1 and 2, optimized  $f_n$ -*FDR* could increase or decrease  
343 along these periods. The optimization ranges for the *FDR* were different and decreased  
344 from period 2 to period 3. Accordingly, optimized  $f_n$ -*FDR* was expected to decrease from  
345 period 2 to period 3.

346 Optimized values for  $k$ -*FDR*,  $k$ -*SDR*,  $L_0$ -*FDR*,  $L_0$ -*SDR* were, 0.363 yr<sup>-1</sup>, 0.085 yr<sup>-1</sup>, 115 m<sup>3</sup>  
347 CH<sub>4</sub> Mg<sup>-1</sup>, 105 m<sup>3</sup> CH<sub>4</sub> Mg<sup>-1</sup>, respectively. Moreover, the optimized values for  $f_1$ -*FDR*,  $f_2$ -  
348 *FDR* and  $f_3$ -*FDR* were 11%, 70% and 5%, respectively. Contrary to the Six-Variable  
349 Scenario, there is no mismatch between optimized *FDR* and *SDR* fractions and the history  
350 of refuse admittance. The value of optimized  $k$ -*SDR* is nearly four times lower than that of

351  $k$ - $FDR$  and the value of optimized  $L_0$ - $SDR$  is moderately higher than that of  $L_0$ - $FDR$ .  
352 According to the Seven-Variable Scenario, the MTT would be reached by 2027.

353

354 The Seven-Variable Scenario allows for consideration of changes in landfilling trends, as  
355 reflected in variations of  $FDR$  and  $SDR$  fractions. This is a clear added-value to the simple  
356 phase Two-Variable Scenario. In addition, contrary to the Six-Variable Scenario, the  
357 optimized variables of the Seven-Variable Scenario better reflect the landfilling history.  
358 For these reasons, the year 2027 – when the Seven-Variable Scenario is expected to reach  
359 the MTT – is a more reliable prediction for gas collection shutdown. Figure 5 shows MTT  
360 for the Two- and Seven-Variable Scenarios.

361

362 Figure 5 – Minimum Technological Threshold for the Two- and the Seven-Variable  
363 Scenarios.

364

### 365 **Effect of the variation of landfill gas recovery efficiency**

366 The results presented above were obtained by adopting 75% recovery efficiency  
367 throughout the lifetime of the CESM landfill. The effect of recovery efficiency on the MTT  
368 year of occurrence and on the SSE for the three scenarios was tested by varying it from  
369 55% to 95% in increments of 10 percentage points. At each increment, a new optimization  
370 was performed for each scenario. The results obtained are presented in Figure 6, which  
371 shows that when the recovery efficiency is increased from 75% to 95%, the MTT occurs

372 1, 3 and 2 years earlier, for the Two-, Six- and Seven-Variable Scenarios, respectively. For  
373 all practical purposes, these differences can be considered relatively small. The results of  
374 Figure 6 also show that, regardless of the value of the recovery efficiency, the Six-Variable  
375 Scenario consistently had the lowest SSE. The decrease in SSE becomes smaller as  
376 recovery efficiency increases and seems to level off when the recovery efficiency reaches  
377 75%.

378 Although not apparent in the results presented in Figure 6, our analyses show that for all  
379 tested efficiencies, the Seven-Variable Scenario seemed to better reflect the landfilling  
380 history at the Montreal-CESM landfill, while the Six-Variable Scenario presented the same  
381 discrepancy between optimized values and landfilling history, as previously mentioned.

382 High LFG recovery efficiencies are expected in this landfill due to the more than 250  
383 biogas collection wells installed. Numerous surface and lateral migration surveys have  
384 shown that surface fluxes have been very low. It is up to the operator to consider the  
385 efficiency level he/she feels comfortable with when estimating the year of occurrence of  
386 MTT for this particular site.

387

388 Figure 6 – MTT year of occurrence (a) and SSE (b) as a function of recovery efficiency.

389

390 **Effect of start of transition year between periods 1 and 2**

391 The sensitivity of the choice made for the transition year between periods 1 and 2 – when  
392 recycling programs became effective, therefore affecting landfilled *FDR* and *SDR* fractions  
393 – was assessed for the Seven-Variable Scenario and for 95% recovery efficiency. Figure 7  
394 shows the effect of moving the end-of-period four years back or forward, relative to 1990.  
395 As the limit year was moved from 1986 to 1994, there was a minimal effect on modeled  
396 generation values after the generation peak.

397

398 Figure 7 - Effect of the variation of the limit year between periods 1 and 2 on the  
399 modeling of CH<sub>4</sub> generation for the Seven-Variable Scenario.

400

#### 401 **FURTHER DISCUSSIONS AND LIMITATIONS**

402 The method proposed in this study accounts for the variation in the nature of admitted  
403 refuse at landfill sites, which is a consequence of changes in the environmental  
404 consciousness of societies – in turn reflected in stricter regulations – and the economics of  
405 waste management. Consideration of how these socio-economic changes affect landfill gas  
406 generation is crucial when it comes to making decisions about the fate of systems put in  
407 place to reduce the environmental impact of landfills and increase their economic viability.

408 Errors associated with measurements of various gas concentrations at the CESM landfill  
409 can be considered minor, due, in part, to continuous gas quality monitoring and the quality  
410 control assured by the well-equipped laboratory on site. However, high operational  
411 variances may have caused the bumps in the generation curve observable in the years 2000

412 and 2012 (Figure 4). These variances can be attributed to a myriad of causes, including: re-  
413 excavation and re-landfilling of waste, temporary difficulties with the gas or leachate  
414 collection systems (such as defective wells), localized settlements, localized elevated  
415 temperatures, etc. Consideration of variable recovery efficiency could account, at least in  
416 part, for the operational variances; hence the interest in considering it in further works. As  
417 shown in this study, these limitations did not seem to influence the fact that the Seven-  
418 Variable Scenario was found to be the most appropriate scenario to estimate shutdown  
419 time, despite the fact that its minimization error was not the lowest.

420

## 421 **ACKNOWLEDGEMENTS**

422 This study received financial support from the Université de Sherbrooke's Center of  
423 Excellence GREEN-TPV, and the Natural Science and Engineering Research Council of  
424 Canada (NSERC), under Discovery Grants RGPIN-170226-2013 and  
425 RGPIN-402368-2011.

426

## 427 **REFERENCES**

428 Baillargeon, A., Bisson, M., Blouin, V., Mercure, A., Séguin, M., Guimond, J.Y., 2006.  
429 Characterization study of the wastes landfilled at CESM (in French: Étude de  
430 caractérisation des chargements entrant au CESM). City of Montreal (Ville de Montreal),  
431 Montreal, QC, p. 21.

432 De la Cruz, F.B., Barlaz, M.A., 2010. Estimation of waste component-specific landfill  
433 decay rates using laboratory-scale decomposition data. *Environ. Sci. Technol.* 44,  
434 4722–4728.

435 Franzidis, J.P., Héroux, M., Nastev, M., Guy, C., 2008. Lateral Migration and Offsite  
436 Surface Emission of Landfill Gas at City of Montreal Landfill Site. *Waste Management &*  
437 *Research* 26, 121-131.

438 Héroux, M., 2008. Développement d'outils de gestion des biogaz produits par les lieux  
439 d'enfouissement sanitaire (in French. Translation of title: Development of Landfill Biogas  
440 Management Tools), *Génie minéral. École Polytechnique de Montréal, Montreal, Quebec,*  
441 p. 281.

442 Héroux, M., Guy, C., Millette, D., 2010. A Statistical Model for Landfill Surface  
443 Emissions. *Journal of Air & Waste Management Association* 60, 219-228.

444 IPCC, 2006. Guidelines for National Greenhouse Gas Inventories, in: Eggleston, S.,  
445 Buendia, L., Miwa, K., Ngara, T., Tanabe, K. (Eds.), Hayama, Japan.

446 Lagos, D.A., 2014. Optimisation du modèle de génération de méthane du lieu  
447 d'enfouissement du complexe environnemental de Saint-Michel, CUFÉ. Université de  
448 Sherbrooke, Sherbrooke, p. 80.

449 RECYC-QUÉBEC, 2000. Bilan 2000 de la gestion des matières résiduelles au Québec, p.  
450 30.

451 Spokas, K., Bogner, J., Chanton, J.P., Morcet, M., Aran, C., Graff, C., Golvan, Y.M.-L.,  
452 Hebe, I., 2006. Methane mass balance at three landfill sites: What is the efficiency of  
453 capture by gas collection systems? *Waste Management* 26, 516-525.

454 Spokas, K., Bogner, J., Corcoran, M., Walker, S., 2015. From California dreaming to  
455 California data: Challenging historic models for landfill CH<sub>4</sub> emissions. *Elementa: Science*  
456 *of the Anthropocene* 3, 16.

457 Thompson, S., Sawyer, J., Bonam, R., Valdivia, J.E., 2009. Building a better methane  
458 generation model: Validating models with methane recovery rates from 35 Canadian  
459 landfills. *Waste Management* 29, 2085-2091.

460 USEPA, 2005. Landfill Gas Emissions Model (LandGEM) Version 3.02 User's Guide.  
461 United States Environmental Protection Agency, Washington, D.C., p. 56.

462 Wang, X., Nagpure, A.S., DeCarolis, J.F., Barlaz, M.A., 2013. Using Observed Data to  
463 Improve Estimated Methane Collection from Select U.S. Landfills. *Environmental Science*  
464 *and Technology* 47, 3251-3257.

465 Wang, X., Padgett, J.M., De la Cruz, F.B., Barlaz, M.A., 2011. Wood Biodegradation in  
466 Laboratory-Scale Landfills. *Environ. Sci. Technol.* 45, 6864-6871.

467

468

469 List of Tables

470

471

472

473

474

475

476

477

478

Type of Waste		Climate Zone <sup>a</sup>								
		Boreal and Temperate (MAT ≤ 20°C)				Tropical <sup>1</sup> (MAT > 20°C)				
		Dry (MAP/PET < 1)		Wet (MAP/PET > 1)		Dry (MAP < 1000 mm)		Moist and Wet (MAP ≥ 1000 mm)		
		Default	Range <sup>2</sup>	Default	Range <sup>2</sup>	Default	Range <sup>2</sup>	Default	Range <sup>2</sup>	
<i>SDR</i>	Slowly degrading waste	Paper/textiles waste	0.04	0.03 <sup>3,5</sup> – 0.05 <sup>3,4</sup>	0.06	0.05 – 0.07 <sup>3,5</sup>	0.045	0.04 – 0.06	0.07	0.06 – 0.085
	Wood/ straw waste		0.02	0.01 <sup>3,4</sup> – 0.03 <sup>6,7</sup>	0.03	0.02 – 0.04	0.025	0.02 – 0.04	0.035	0.03 – 0.05
<i>FDR</i>	Moderately degrading waste	Other (non – food) organic putrescible/ Garden and park waste	0.05	0.04 – 0.06	0.1	0.06 – 0.1 <sup>8</sup>	0.065	0.05 – 0.08	0.17	0.15 – 0.2
	Rapidly degrading waste	Food waste/Sewage sludge	0.06	0.05 – 0.08	0.185 <sup>4</sup>	0.1 <sup>3,4</sup> – 0.2 <sup>9</sup>	0.085	0.07 – 0.1	0.4	0.17 – 0.7 <sup>10</sup>

} *Max = 0.085*  
} *Min = 0.03*

} *Max = 0.7*  
} *Min = 0.15*

479 Table 1 - Segregation of *FDR* and *SDR* and corresponding k values as per IPCC  
480 recommended ranges. Adapted from IPCC (2006).

481

	Optimization range for $k$ (yr <sup>-1</sup> )	Optimization range for $L_0$ (m <sup>3</sup> CH <sub>4</sub> Mg <sup>-1</sup> )
Two-Variable Scenario	[0.030–0.700]	[21–241]
Six-Variable Scenario	[0.030–0.700]	[21–241]
Seven-Variable Scenario	<i>FDR</i> [0.100–0.700]	[21–115]
	<i>SDR</i> [0.030–0.085]	[105–241]

482

483 Table 2 -  $k$  and  $L_0$  optimization ranges for the Two-, Six- and Seven-Variable Scenarios  
484 (Based on IPCC (2006) values).

485

486

487



Period	Optimization range for landfilled <i>FDR</i> fraction (%)
1: 1968–1989	[10–50]
2: 1990–1999	[30–70]
3: 2000–2008	[0–10]

488

489 Table 3 - Optimization ranges for FDR fractions in the Seven-Variable Scenario for the

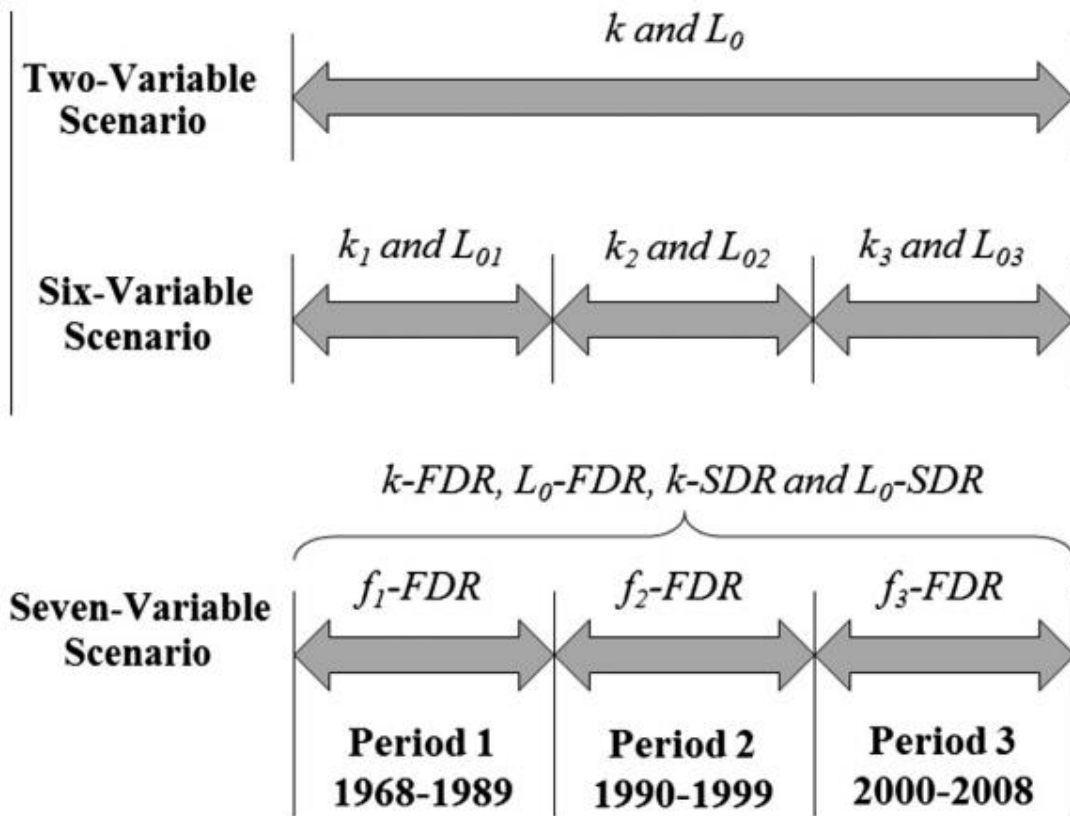
490 three periods considered.

491

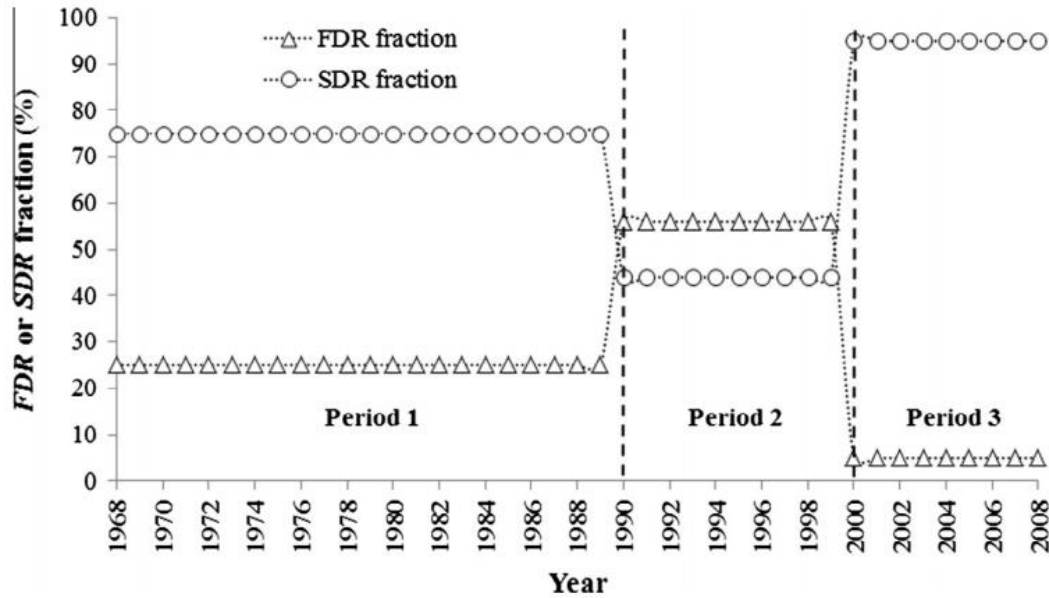
492

493

494



498 Figure 1 - Schematic of the three scenarios and their corresponding variables.

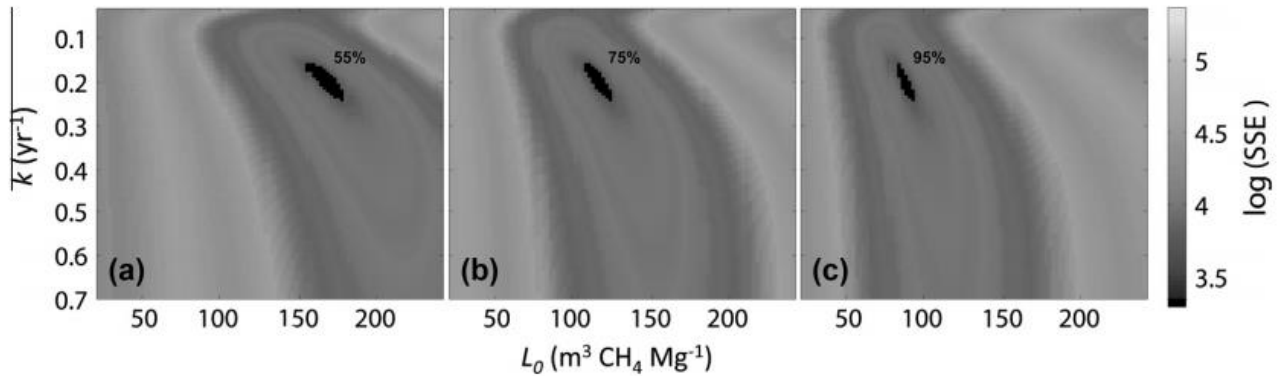


500

501 Figure 2 - Schematic representation of the evolution of estimated *FDR* and *SDR* fractions

502 at CESM from opening (1968) to closure (2008).

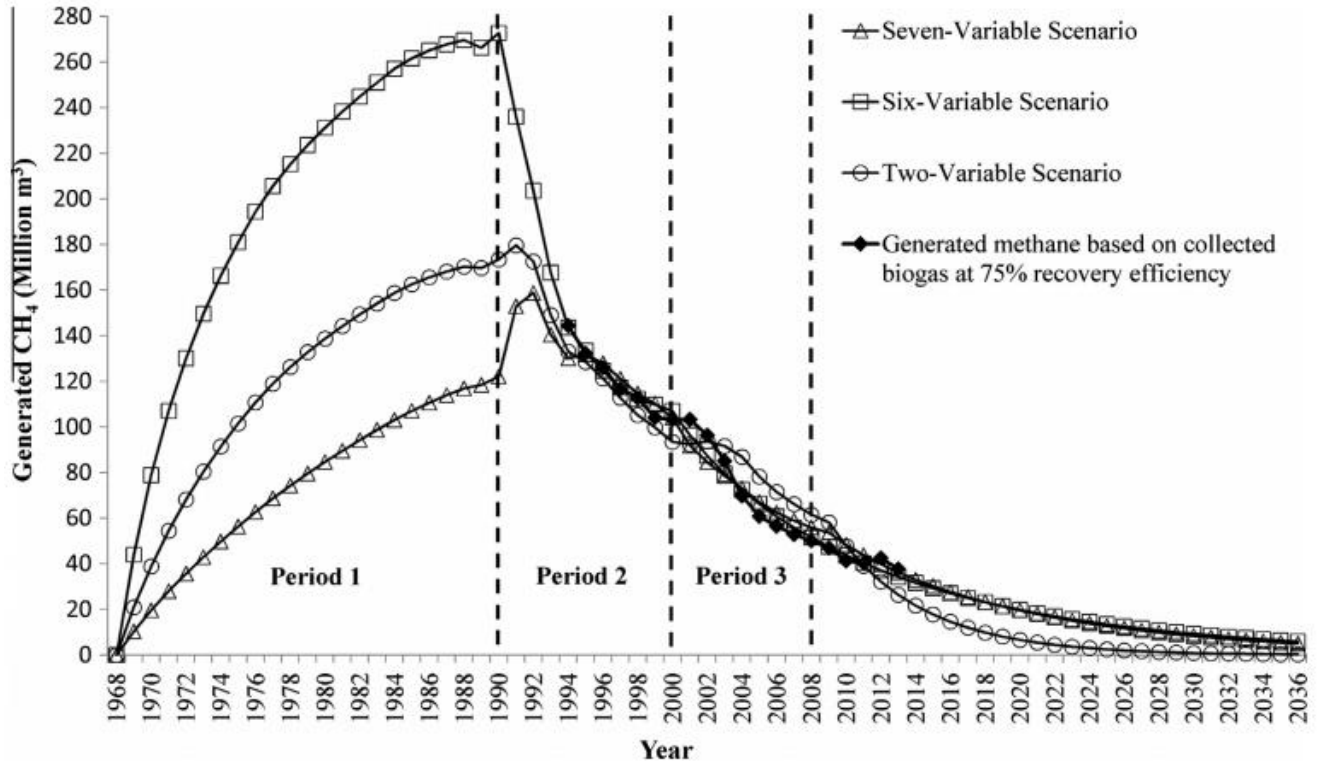
503



504

505 Figure 3 – Model-predicted errors for the Two-Variable Scenario as function of recovery

506 efficiency.



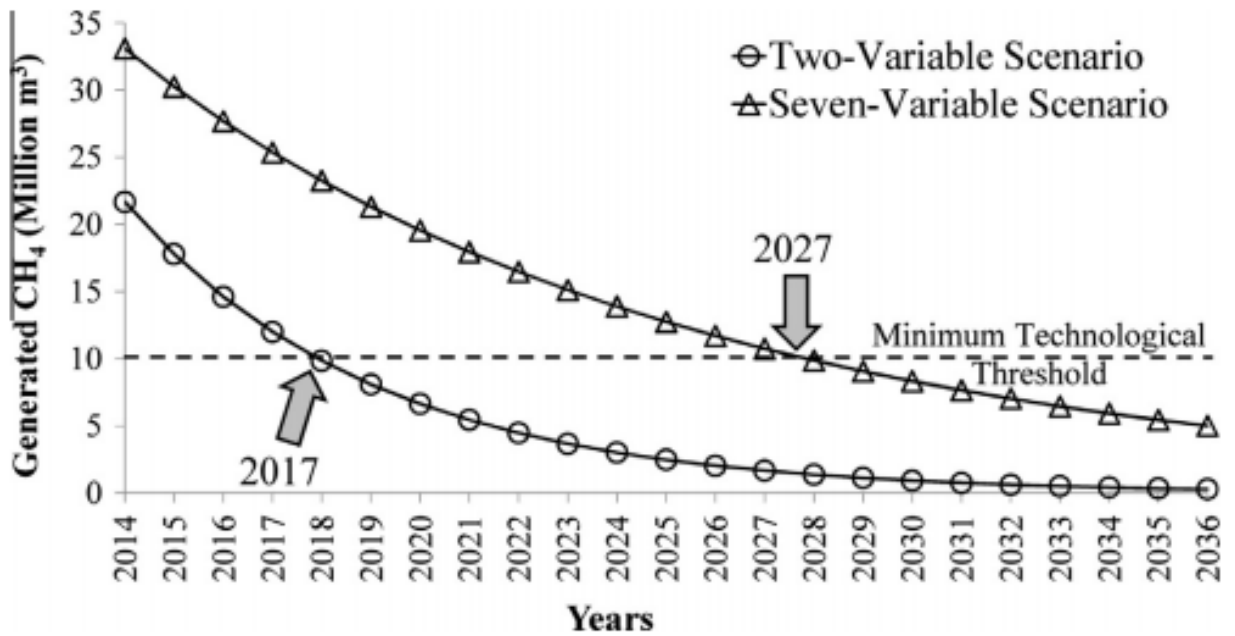
507

508 Figure 4 - Modeled CH<sub>4</sub> generation for the Two-, Six- and Seven-Variable Scenarios as  
 509 optimized after SSE minimization relative to measured CH<sub>4</sub> generation.

510

511

512

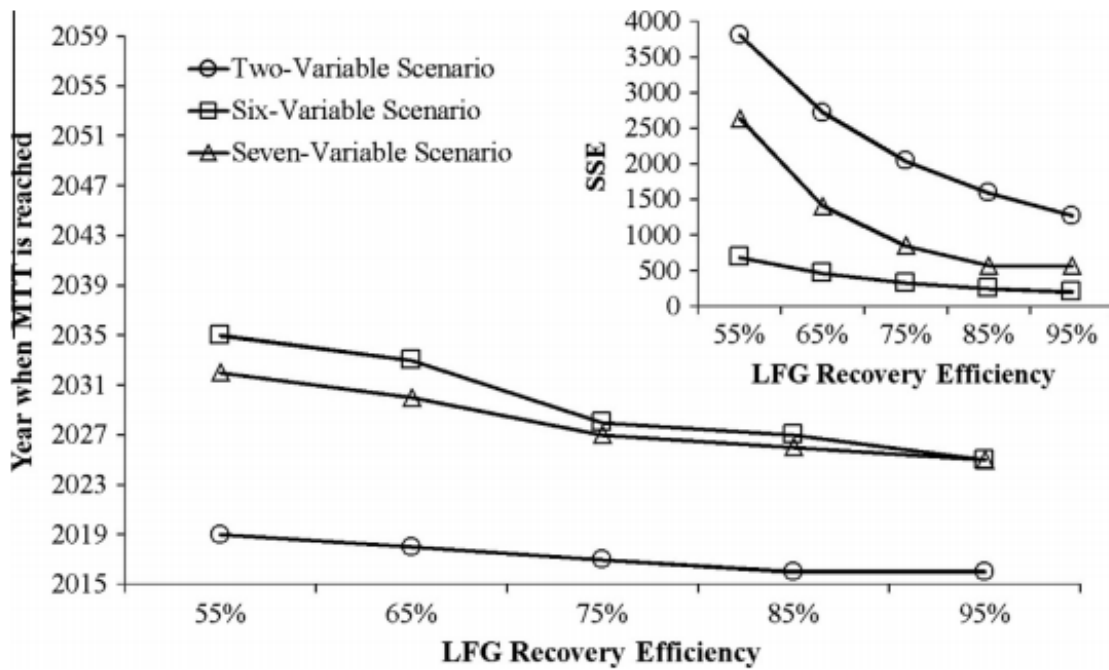


513

514 Figure 5 – Minimum Technological Threshold for the Two- and the Seven-Variable

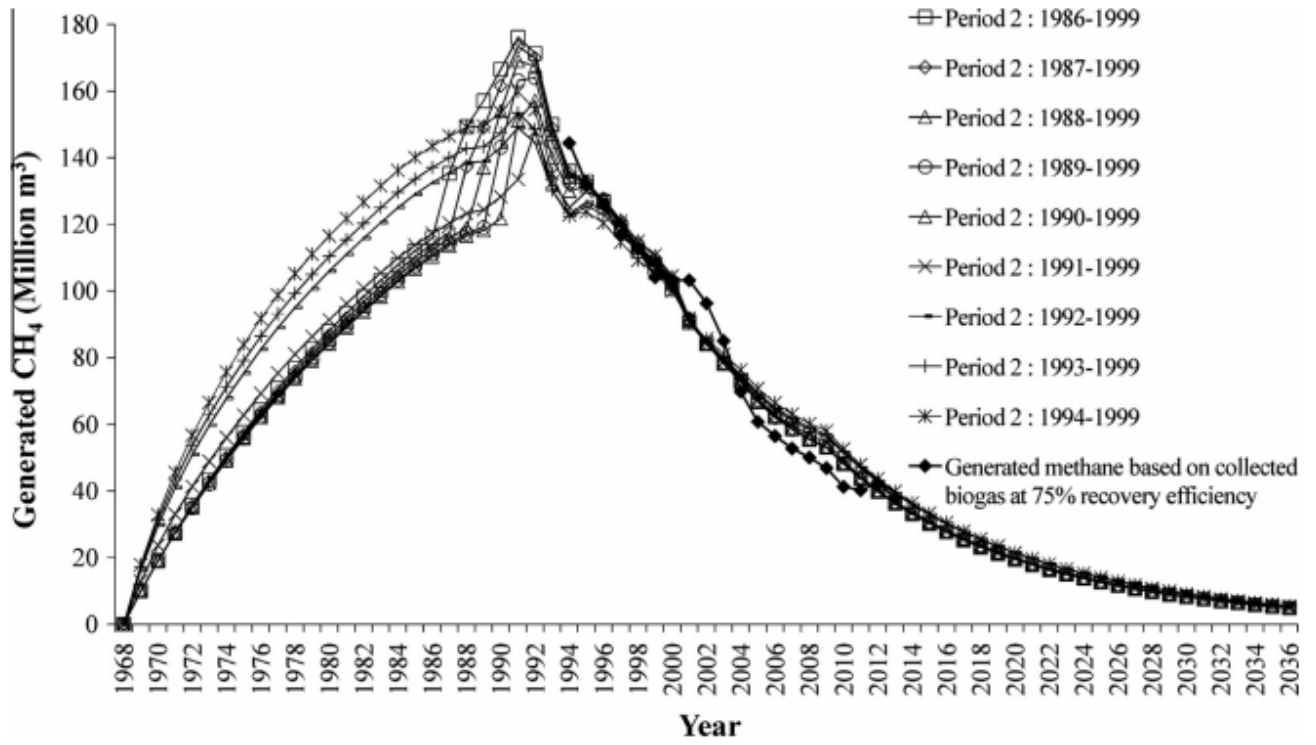
515 Scenarios.

*D.A. Lagos et al./Waste Management xxx (2016) xxx-xxx*



516

517 Figure 6 – MTT year of occurrence (a) and SSE (b) as a function of recovery efficiency.



518

519 Figure 7 - Effect of the variation of the limit year between periods 1 and 2 on the  
 520 modeling of CH<sub>4</sub> generation for the Seven-Variable Scenario.